A finite element simulation on creep behavior in welded joint of chrome-molybdenum steel including interaction between void evolution and dislocation dynamics

T. Iwamoto, E. Murakami, T. Sawa

This paper deals with a new framework of a numerical method for a prediction of creep behavior in a welded joint with a chrome-molybdenum steel by including both void evolution and dislocation dynamics. For a creep constitutive equation with void evolution, the model proposed in the past is generalized by vanishing the locally coupled analysis. A dislocation model with a scalar variable of dislocation density, which the dislocation can be piled up and annihilated, is included into the creep constitutive equation. Interactions between the void and dislocation are newly considered, as the void becomes an obstacle against the dislocation motion and a dense dislocation field becomes a source and a sink of the void.

1 Introduction

A coal-fired boiler is taking an important role of an electric power generation. The boiler is still major energy source, however, firing the coal with a huge emission of carbon dioxide is not good selection since the carbon emission should be reduced rapidly for maintaining the environment from the recent requirement. Instead of a conventional power plant, a ultra super critical (USC) coal power plant has been developed for increasing an efficiency of energy and decreasing the carbon emission. Figure 1 shows a shift in coal-fired boilers and materials used for them (Bao, 2007). In USC boilers, higher efficiency can be obtained and the steam condition becomes quite strict instead. The material used for them is strongly required to endure such the strict condition. Now, two kinds of materials are employed for boilers as shown in the figure. One is a chrome-molybdenum steel, which is employed mostly.

In many cases, this steel is heat-treated to increase its creep strength. However, the creep strength of a heat-

Figure 1: Shift in coal-fired boilers and materials used for them

affected zone (HAZ) created after welding at the welded joint of the steel is quite low. Figure 2 (a) shows a hardness distribution through the welded joint (Bao, 2007). As shown in this figure (a), the hardness suddenly decrease at the HAZ near the interface between the HAZ and the base metal. According to an analogy from the hardness distribution, it is possible that a failure originates from the HAZ near the interface due to decrease of its creep strength. Figure 2 (b) shows a photograph of a cross-section of a specimen after the creep failure in the welded joint (Bao, 2007). As shown in this figure, the fracture occurs at the HAZ near the interface. This result is corresponding the hardness distribution. This fact is a huge problem for a reliability of the USC coal power plant. To improve the reliability of USC boilers, an increase of its creep strength might become a key technology and a prediction of its creep strength is quite essential.

Figure 3 shows micrographs of a cross-section in the HAZ at (a) 10 mm, (b) 40 mm in depth from the surface and (c) growth to a crack after a coalescence of voids (Hasegawa and Maeda, 2006). As shown in this figure, a microvoid is nucleated at different locations in the HAZ and the number of voids inside the HAZ becomes larger as compared with that near the surface. A coalescence of the voids can be observed and this coalescence
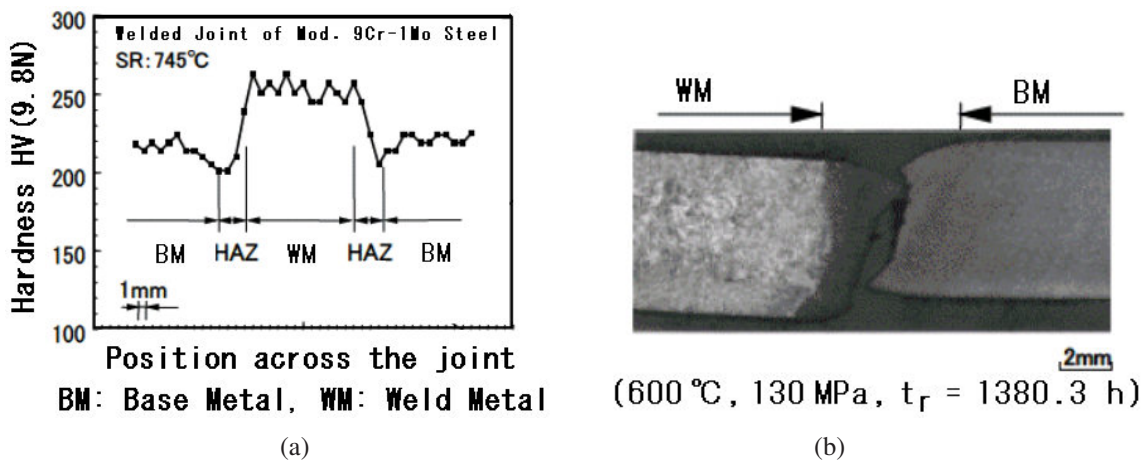

Figure 2: (a) Hardness profile through the welded joint and (b) a photograph of a cross-section of a specimen after the creep failure in the welded joint of the chrome-molybdenum steel
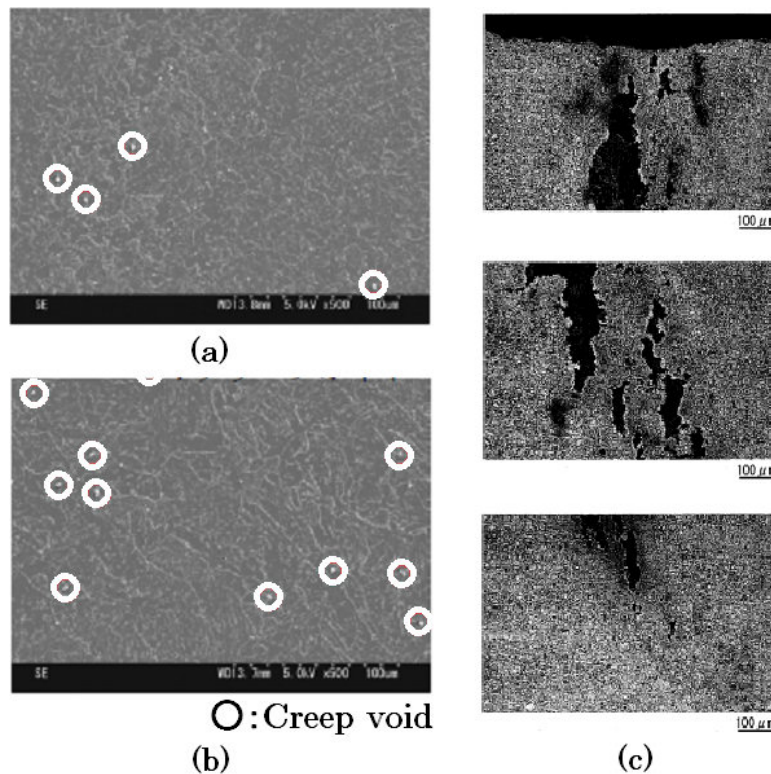

Figure 3: Micrographs of cross-section in the HAZ at (a) 10 mm in depth, (b) 40 mm in depth from the surface and (c) growth to a crack after a coalescence of voids

is growing to a larger-scaled crack. This consequent process with the nucleation, the growth and the coalescence of the microvoid in the HAZ is a main mechanism of the decrease in its creep strength. Therefore, a prediction and a control of a damage due to the creep void evolution is quite essential to prevent a failure of the boilers and increase their lifetime. In order to predict the creep void evolution, Takemasa et al. (1999) proposed that a creep constitutive equation based on the Tvergaad-Needleman model (Tvergaard and Needleman, 1984), which was originally developed for the ductile fracture analysis of porous materials by extending the Gurson's model (Gurson, 1977). They introduced the locally coupled analysis (Lemaitre, 1996). As Lemaitre said in this book, this analysis is effective for brittle and fatigue types of damage. Hence, we have a doubt that this analysis can be applied for the creep behavior or not. Furthermore, although their FE calculation by using the commercial FE software ABAQUS shows that the creep strain is not localized near the interface between the HAZ and the base metal, the void fraction calculated on the basis of the computational result is strongly localized there.

Here, a new framework for a numerical analysis of creep behavior including both a void evolution and a dislocation dynamics for a modified 9Cr-1Mo steel welded joint is proposed. First, the creep constitutive model with the void evolution proposed by Takemasa et al. Takemasa et al. (1999) is generalized by vanishing the locally coupled analysis. By using the set of parameters appeared in the article (Takemasa et al., 1999), a simulation with the same condition is performed in order to compare with the computational results obtained by Takemasa et al. (1999). After that, a dislocation model proposed in the past (Mecking and Kocks, 1981; Estrin, 1998) is included into the creep constitutive equation. In this model, the dislocation can be piled up and annihilated. Interactions between the void and the dislocation are newly considered, as the void becomes an obstacle against the dislocation motion and the dense dislocation leads to the source and sink of the microvoid. All the proposed constitutive equations are implemented into the commercial software ABAQUS through the user material subroutine UMAT. The newly proposed model is verified by a comparison with the experimental result. Finally, effects of interactions and the grain size of HAZ considered here on distribution of a void fraction, a dislocation density and creep strain are examined.

2 Fundamental theory

In this section, the three different models of the creep potential, the void evolution and the dislocation dynamics are individually explained. Of course, models for interactions between void and dislocation are described here.

2.1 Gurson's creep potential

Gurson (1977) originally developed the model for the ductile fracture analysis of porous materials. And then, Tvergaard and Needleman (1984) extended Gurson's model and the well-known Tvergaad-Needleman model is widely used in order to solve problems related to the ductile fracture and/or porous materials. Obeying Takemasa et al. (1999), a plastic deformation in their model is automatically replaced to a creep deformation.

First, the total strain rate $\dot{\varepsilon}_{ij}$ can be decomposed into three parts as

$$\dot{\varepsilon}_{ij} = \dot{\varepsilon}_{ij}^e + \dot{\varepsilon}_{ij}^t + \dot{\varepsilon}_{ij}^c. \tag{1}$$

$\dot{\varepsilon}_{ij}^e$ and $\dot{\varepsilon}_{ij}^t$ are the elastic and the thermal parts of the strain rate which can be expressed by

$$\dot{\varepsilon}_{ij}^e = B_{ijkl}\dot{\sigma}_{ij} \text{ and } \dot{\varepsilon}_{ij}^t = \kappa_{ij}\dot{T}, \tag{2}$$

where B_{ijkl} is the elastic compliance tensor, $\dot{T}$ is a rate of temperature and κ_{ij} is the thermal expansion tensor. If a thermally-isotropic material is considered, κ_{ij} becomes the simple form of $\alpha_T \delta_{ij}$, where α_T is the thermal expansion coefficient. On the other hand, $\dot{\varepsilon}_{ij}^c$ is the creep strain rate and can be formulated obeying the flow rule as

$$\dot{\varepsilon}_{ij}^c = \dot{\lambda}\frac{\partial \Phi}{\partial \sigma_{ij}}. \tag{3}$$

Here, the Gurson's yield function is employed for the creep potential Φ to express the creep deformation with the void evolution as

$$\Phi(\sigma_{ij}, \bar{\sigma}, f_v) = \frac{3}{2}\frac{\sigma'_{ij}\sigma'_{ij}}{\bar{\sigma}^2} + 2q_1 f_v \cosh\left(\frac{3q_2\sigma_m}{2\bar{\sigma}}\right) - \left\{1 - (q_1 f_v)^2\right\} = 0, \tag{4}$$

where f_v indicates the void volume fraction, $\bar{\sigma}$ means the equivalent stress of the fully dense matrix material, σ_m is the hydrostatic stress, q_1 and q_2 are constants. The evolution of the equivalent creep strain in the matrix material is obtained from the following equivalent irreversible work expression by creep:

$$(1 - f_v)\bar{\sigma}\dot{\bar{\varepsilon}} = \sigma_{ij}\dot{\varepsilon}_{ij}^c, \tag{5}$$

where $\dot{\bar{\varepsilon}}$ means the equivalent creep strain of a matrix material. From equations (3) to (5), $\dot{\varepsilon}_{ij}^c$ can be explicitly written as

$$\dot{\varepsilon}_{ij}^c = \frac{(1 - f_v)\bar{\sigma}\dot{\bar{\varepsilon}}}{2\sigma_e^2 + 3q_1 q_2 f_v \bar{\sigma}\sigma_m \sinh\left(\frac{3q_2\sigma_m}{2\bar{\sigma}}\right)}\left\{3\sigma'_{ij} + q_1 q_2 f_v \bar{\sigma}\sinh\left(\frac{3q_2\sigma_m}{2\bar{\sigma}}\right)\delta_{ij}\right\}. \tag{6}$$

As expressed in equation (4), the creep potential has the nonlinear form against $\bar{\sigma}$ and it is hard to obtain an equation for $\bar{\sigma}$. Instead of a use of equation (4), the following equation should be satisfied during the creep deformation as

$$\dot{\Phi} = 0, \tag{7}$$

then we have the following evolution equation for $\bar{\sigma}$ as

$$\dot{\bar{\sigma}} = \frac{A_{ij}\dot{\sigma}_{ij} + B\dot{f}_v}{\frac{2\sigma_e^2}{\bar{\sigma}} + 3q_1 q_2 f^v \sigma_m \sinh\left(\frac{3q_2\sigma_m}{2\bar{\sigma}}\right)}, \tag{8}$$

$$A_{ij} = 3\sigma'_{ij} + q_1 q_2 f_v \bar{\sigma}\sinh\left(\frac{3q_2\sigma_m}{2\bar{\sigma}}\right)\delta_{ij} \text{ and } B = 2q_1\bar{\sigma}^2\cosh\left(\frac{3q_2\sigma_m}{2\bar{\sigma}}\right) - 2q_1^2 f_v \bar{\sigma}^2$$

Since $\bar{\sigma}$ is a function of $\dot{\bar{\varepsilon}}$, Norton's power law is frequently employed for the relationship.

2.2 Void evolution

A rate of total void volume fraction can be generally decomposed into three parts as (Tvergaard and Needleman, 1984; Takemasa et al., 1999)

$$\dot{f}_v = \dot{f}_v^n + \dot{f}_v^g + \dot{f}_v^c. \tag{9}$$

Here, $\dot{f}_v^c$ is the coalescence part of the rate of the void volume fraction and we vanish this term here. $\dot{f}_v^g$ is the rate of void volume fraction concerning with a void growth. Growth of pre-existing or newly-nucleated voids is based on the law of conservation of mass and is expressed in terms of the void volume fraction:

$$\dot{f}_v^g = (1 - f_v)\dot{\varepsilon}_{kk}^c. \tag{10}$$

$\dot{f}_v^n$ is the nucleation part of the void volume fraction. The nucleation of voids is given by a strain-controlled relationship (Chu and Needleman, 1980):

$$\dot{f}_v^n = \frac{F_h}{S_N\sqrt{2\pi}}\exp\left\{-\frac{1}{2}\left(\frac{\bar{\varepsilon} - \varepsilon_N}{S_N}\right)\right\}\dot{\bar{\varepsilon}}. \tag{11}$$

The normal distribution of the nucleation strain has a mean value ε_N and standard deviation S_N. F_h is the volume fraction of the nucleated voids, and voids are nucleated only in tension. The function f^* models the rapid loss of stress carrying capacity that accompanies void coalescence instead of a use of $\dot{f}_v^c$. This function is defined in terms of the void volume fraction:

$$f^* = \begin{cases} f_v & \text{for } f_v \leq f_{cr} \\ f_{cr} + \frac{\frac{1}{q_1} - f_{cr}}{f_F - f_{cr}}(f_v - f_{cr}) & \text{for } f_v > f_{cr} \end{cases}. \tag{12}$$

In the above relationship, f_{cr} is a critical value of the void volume fraction and f_F is the value of void volume fraction at which there is a complete loss of stress carrying capacity in the material. The user-specified parameters

f_{cr} and f_F model the material failure when $f > f_{cr}$, due to mechanisms such as micro fracture and void coalescence. After the substitution of Eqs. (10) and (11) into Eq. (9), the total void volume fraction f_v can be calculated by a time integration of Eq. (9). Then, the above function f^* is applied for on the basis of the calculated f_v.

2.3 Evolution of dislocation density

Mecking and Kocks (1981) proposed the model for a strain-hardening in terms of the dislocation density as

$$\sigma_0 = M\alpha Gb\sqrt{\rho}, \tag{13}$$

where M is the Taylor factor, G is the shear modulus, b is the magnitude of the Burger's vector, ρ is the dislocation density and α is a constant. In order to express the strain hardening behavior with the evolution of dislocation density by using the above equation, the conventional Norton's power law is modified as (Estrin and Mecking, 1984)

$$\dot{\bar{\varepsilon}} = A\left(\frac{\bar{\sigma}}{\sigma_0}\right)^m, \tag{14}$$

where A is a constant and m is the strain rate sensitivity exponent. The form of the equation for the evolution of the dislocation density makes it possible to include in the model of the metallurgical characteristics as well as information on the microstructure of the material. The evolution law of the dislocation density takes into account of a storage as well as an annihilation of dislocation. The time evolution of ρ in the process of creep deformation is described as Mecking and Kocks (1981), and Estrin (1998)

$$\dot{\rho} = M\left(\frac{1}{\Lambda b} - k\rho\right)\dot{\bar{\varepsilon}}, \tag{15}$$

where Λ is the mean free path of the dislocation. The first term in the bracket on the right hand side of the above equation characterizes the processes of storage for dislocations. The second term is related to the annihilation and expresses the thermally activated process of dynamic recovery during the creep deformation. The coefficient k characterizes the concurrent dislocation annihilation and represents the thermally activated process by a dislocation cross-slip at low temperature or a dislocation climb at high temperature. The strain rate dependence of k can be expressed as

$$k = k_0\left(\frac{\dot{\bar{\varepsilon}}}{\dot{\bar{\varepsilon}}_0}\right)^{-\frac{1}{\ell}}. \tag{16}$$

$\dot{\bar{\varepsilon}}_0$ is the reference strain rate as a function of temperature and ℓ is a constant. In this work, $\dot{\bar{\varepsilon}}_0$ is dealt with as a constant.

Λ is given by the average dislocation spacing. In a more general case of a material with a microstructure, Λ can be expressed as

$$\frac{1}{\Lambda} = \sum_i \frac{1}{\Lambda_i}, \tag{17}$$

where the quantities Λ_i denote the particular values of the mean free path for an individual dislocation storage mechanism. For example, Estrin (1998) employed two kinds of the mean free path as

$$\frac{1}{\Lambda} = \frac{1}{\Lambda_1} + \frac{1}{\Lambda_2} = \frac{1}{d} + \beta\sqrt{\rho}, \tag{18}$$

where, d is the grain size and β is a constant. The first term on the right hand side means effect of grain boundary at the initial state. The second term represents the effect of the dislocation forest. Both effects are acting as obstacles for mobile dislocations.

2.4 Models for interactions between void and dislocation

Once dislocation is piling up at obstacles such as a grain boundary, a harder phase, etc., the possibility of an increase in nuclei of the microvoid might become higher. Hence, it can be assumed that the dislocation evolution affects on the void evolution. Lubarda et al. (2004) proposed a mechanism of void growth by dislocation emission from the surface of the void under a shock loading. Their idea is similar to ours and becomes a valuable evidence to support the assumption described above. This effect can be introduced into the model as the first interaction between void and dislocation evolution. The rate of void volume fraction $\dot{f}_v$ can be decomposed into three parts with an exception of the coalescence term as

$$\dot{f}_v = \dot{f}_v^g + \dot{f}_v^n + \dot{f}_v^D, \tag{19}$$

$\dot{f}_v^D$ means the effect of a dislocation on the nucleation and the growth of the void. Li et al. (2009) proposed the framework which consists of the continuum damage mechanics and the dislocation dynamics established by Mecking and Kocks (1981), and Estrin (1998) to solve a recovery of mechanical properties after annealing of a linepipe including the recrystallization. Obeying Li et al. (2009), the equation for the damage variable is employed to describe the effect and can be expressed as

$$\dot{f}_v^D = C(1 - f_v)\dot{\rho}, \tag{20}$$

where C is a constant.

On the other hand, the void might become an obstacle for the dislocation motion. Serri and Cherkaoui (2008) introduced the third mean free path and employed the explicit form of the mean free path proposed by Fullman (1953) for the simulation of TRIP steels which contains a hard martensitic phase as the obstacle. The idea can be introduced into this framework. To describe this effect, the third mean free path Λ_3 which indicates an interval between the microvoids is introduced into the equation (18) as

$$\frac{1}{\Lambda} = \frac{1}{d} + \beta\sqrt{\rho} + \frac{1}{\Lambda_3} \tag{21}$$

Obeying Fullman (1953), and Serri and Cherkaoui (2008), Λ_3 can be expressed as:

$$\frac{1}{\Lambda_3} = \frac{1}{2e}\frac{f_v}{1 - f_v}, \tag{22}$$

where e is the average radius of the microvoid.

It is noted that all of f_v formulated in this section can be rewritten to f^* to include the effect of the void coalescence.

3 Computational model and conditions

The above-mentioned constitutive models are implemented into the ABAQUS through a user defined material subroutine UMAT based on the implicit time integration. According to the ABAQUS Manual, the time step can be controlled automatically within a certain range of the time which the user can be defined. Figure 4 shows the computational model with FE mesh division and boundary conditions. Creep behavior of the rounded bar specimen with the nominal stress of 49 MPa at the left end is simulated. The specimen is divided into three regions such as a base metal, an HAZ and a weld metal. The size of regions and the specimen is written in the figure. The eight nodes quadratic element is used and the total number of elements is 2325. The FE mesh division becomes finer near interfaces between each material and the circumferential surface. To keep a flat end during the creep deformation, a constraint of nodal displacements for the loading direction is introduced at the left side of edge. The material parameters and constants used here are shown in Table 1. These parameters are determined by the reference of articles published in the past (Takemasa et al., 1999; Serri and Cherkaoui, 2008; Li et al., 2009).

4 Validity of user defined subroutine and calculated results including void and dislocation evolution

Figure 5 shows distribution of (a) von Mises equivalent stress and (b) equivalent creep strain at 7595.4 hrs computed by the ABAQUS with the conventional Norton's law and the established user material subroutine without void
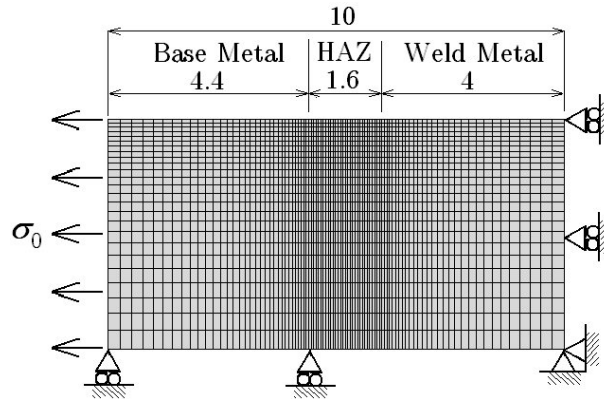
Figure 4: Finite element model with boundary conditions

Table 1: Material parameters and constants used here for the modified 9Cr-1Mo steel

@ / @	Base Metal	HAZ	Weld Metal	@@ / @@	Base Metal	HAZ	Weld Metal
E [GPa]	90000			ν	0.28		
A	8.0×10^{-17}	3.3×10^{-20}	1.3×10^{-15}	m	4.7	6.7	4.2
q_1	1.5			q_2	1.0		
f_F	0.018			f_{cr}	0.01		
F_h	0.035			S_N	0.01		
ε_N	0.03			M	3.06		
α	0.43	0.33	0.43	b [mm]	2.56×10^{-7}		
k_0	7.35		8.23	$\dot{\bar{\varepsilon}}_0$	3.6×10^3		
ℓ	25.0	21.0	22.0	d [mm]	5.0×10^{-3}		
β	3.1×10^{-2}	3.2×10^{-2}	5.3×10^{-2}	ρ_{init} [mm^{-2}]	1.0×10^3		
e [mm]	4.0×10^{-4}			C	1.7×10^{-5}		

and dislocation evolution. The above-mentioned constitutive equation without effects of dislocation and void is equivalent to the Norton's law which has already implemented into the ABAQUS. From this figure, the fairly good agreement can be observed. Thus, the developed UMAT is valid for the further computations with void and dislocation evolution.

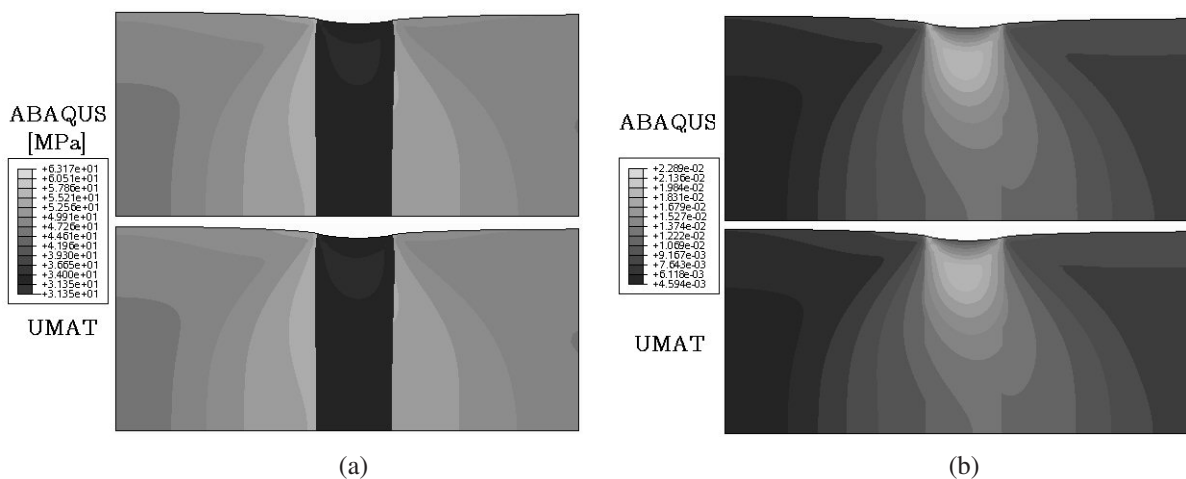(a)   (b)

Figure 5: Distribution of (a) von Mises equivalent stress and (b) equivalent creep strain at 7595.4 hrs computed by the ABAQUS with Norton's law and developed UMAT without void and dislocation evolution

Figure 6 (a) shows the creep curve obtained by the experiment (Fujii et al., 1998a,b) and computation with various constitutive equations. All the computational results are corresponding to the experimental data except for the region of the acceralating creep. In order to confirm in detail, Fig. 6 (b) shows the magnified figure on the vertical
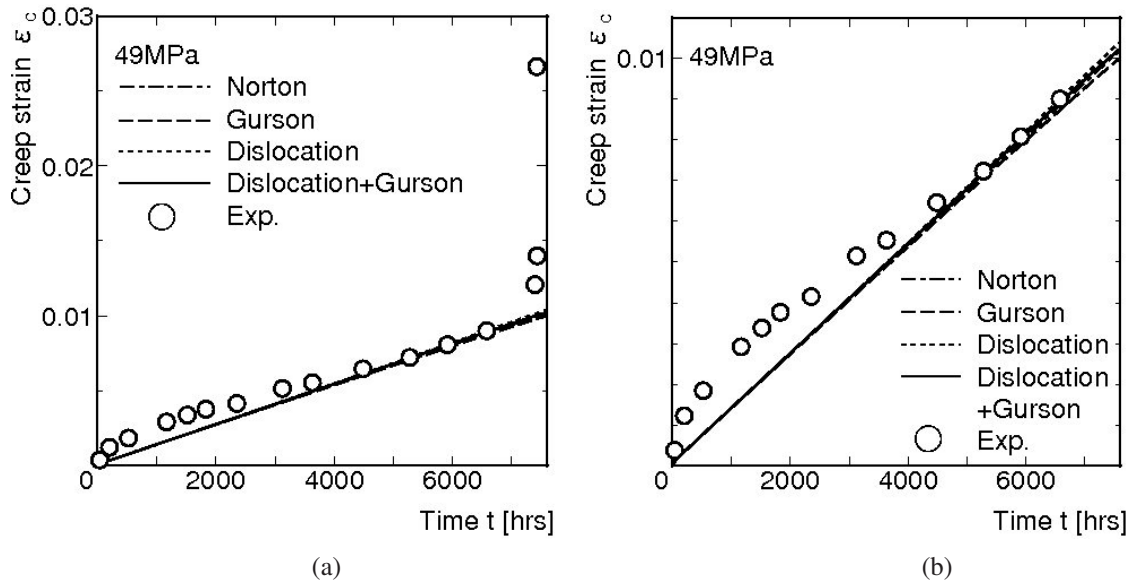
163

Figure 6: (a) Creep curves and (b) their curves maginified on the vertical axis, which are obtained by the experiment and computations calculated with considering void, dislocation evolutions and their interactions.

axis of the figure (a). As shown in this figure, it can be said that the computational result is almost corresponding to the experimental result. However, the difference in the region of the transient creep can be observed. The difference between the computational results with a different constitutive equation is clearly observed in this figure. Thus, the creep curve is affecting on the used constitutive equation slightly. Over 4000 hrs, the difference becomes larger. If only void evolution is considered, the creep strain over 4000 hrs is slightly reduced by a softening effect due to an existence of void. On the other hand, the creep strain slightly increases over 4000 hrs if only dislocation evolution is considered. Computational results with Norton's law and the proposed constitutive equation show a good correspondence by a balance between the softening effect due to a void and the hardening effect due to the dislocation evolution. However, both the primary and the tertiary creep stages are not reproduced by the model. This difference will be able to be vanished by a further study on adjusting the material parameter.

Figure 7 shows distribution of void volume fraction computed by two different kinds of constitutive equation such as (a) Gurson's model (equivalent to the proposed model without dislocation motions) and (b) the model proposed here. As shown in this figure, the void is localized slightly-inside from the surface in the HAZ region. The region with higher void fraction in the base metal near the interface is developed in our calculation including the interaction. Takemasa et al. (1999) reported the void volume fraction becomes maximum inside from the surface near an interface between the HAZ and the base metal from their calculation based on the locally coupled analysis. However, their result can not be seen in this calculation and our result indicates the position of the maximum void fraction is located at the center of the HAZ, not near the interface. It can be said that the locally coupled analysis which they employed is not suitable and some errors are derived.
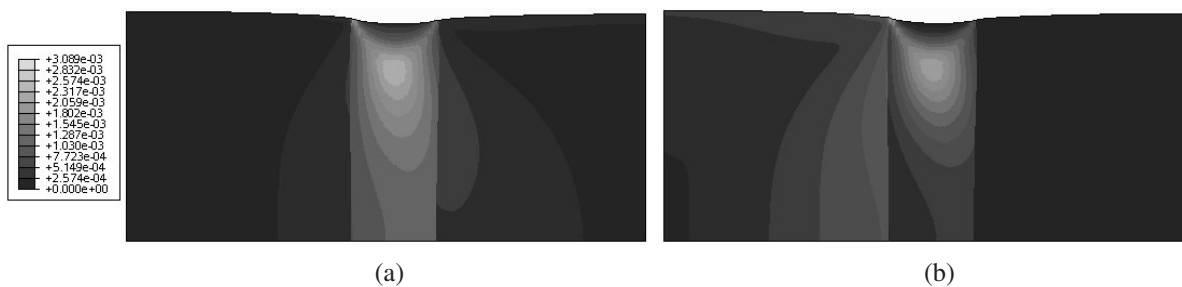

Figure 7: Distribution of void volume fraction calculated by considerations of (a) only void evolution, and (b) an interaction between void and dislocation evolution at 4820 hrs

164

5 Numerical results

In this section, the effect of interactions between void and dislocation evolution is examined. This effect is included into the proposed constitutive equation. Then, the grain size effect included into the mean free path on void evolution is discussed.

5.1 Effect of interactions between void and dislocation

Figure 8 shows creep curves obtained the experiment and computation calculated with a consideration of interactions between void and dislocation evolution. As shown in this figure, creep curves are almost the same and the effect of the interaction on the macroscopic creep behavior is quite small.
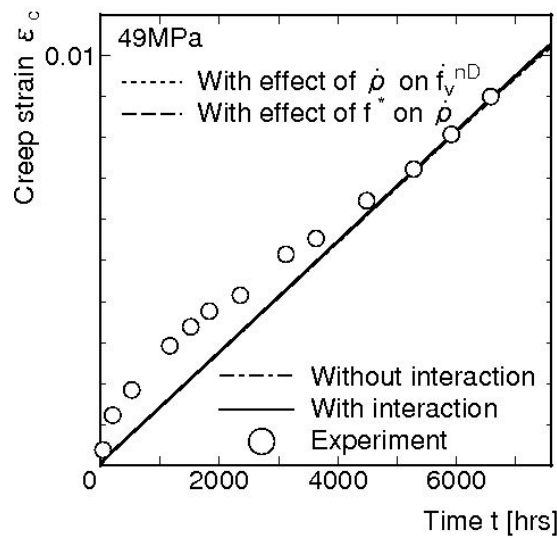

Figure 8: Creep curves obtained by the experiment and computations calculated with a consideration of interactions between void and dislocation evolution.

Figure 9 shows distribution of void volume fraction calculated by considerations of (a) no interaction, (b) only the effect of f^* on $\dot{\rho}$ as expressed in equation (22), (c) only the effect of $\dot{\rho}$ on f_v^D as formulated in equation (20), and (c) both interactions between void and dislocation evolution at 7954.5 hrs. No big difference between the
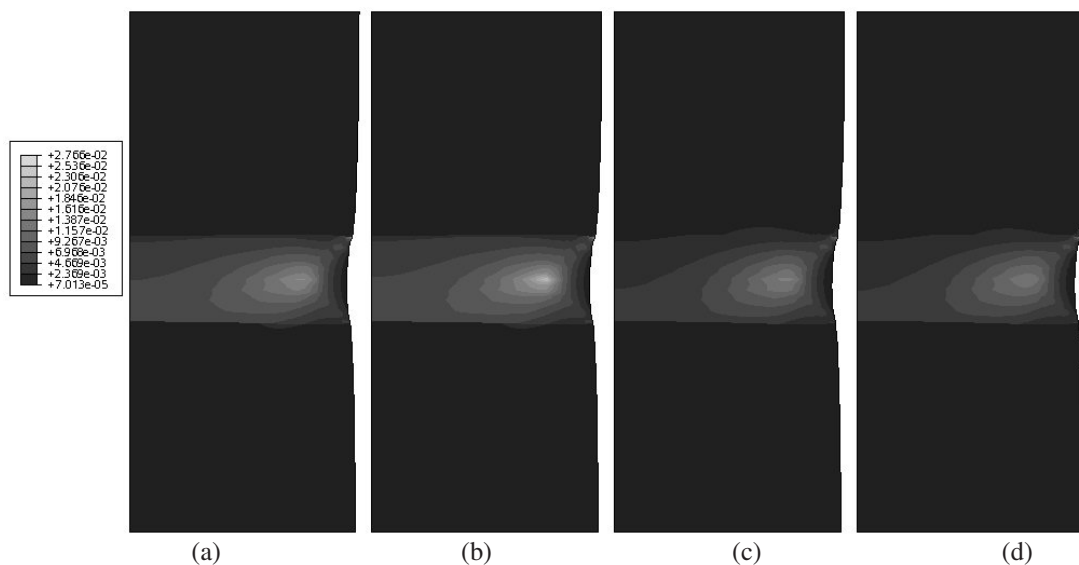

Figure 9: Distribution of void volume fraction calculated by considerations of (a) no interaction, (b) only the effect of f^* on $\dot{\rho}$, (c) only the effect of $\dot{\rho}$ on f_v^D, and (c) both interactions between void and dislocation evolution at 7954.5 hrs
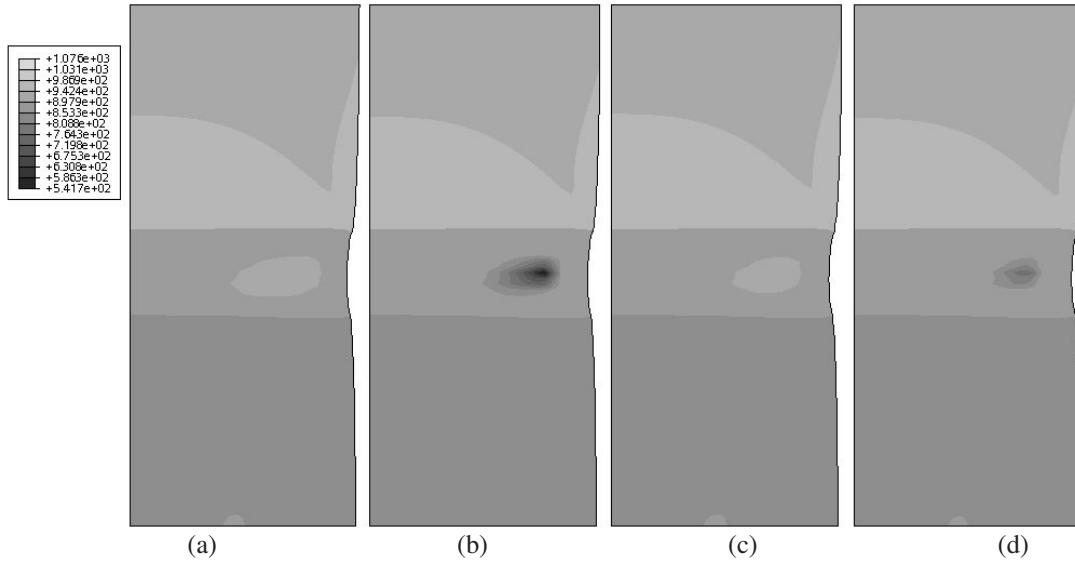
Figure 10: Distribution of dislocation density calculated by considerations of (a) no interaction, (b) only the effect of f^* on $\dot\rho$, (c) only the effect of $\dot\rho$ on f_v^D, and (c) both interactions between void and dislocation evolution at 7954.5 hrs

computational results can be observed, however, the maximum value becomes different. From this figure (b), the maximum value is higher than the case without any interactions because the dislocation is dealt with as a source of void fraction. The shape of distribution as shown in the figure (d) is a kind of sum of distribution as shown in the figures (b) and (c). Mixed feature can be seen as the distribution becomes similar in cases with considerations of no interaction and both interactions.

Figure 10 shows distribution of the dislocation density calculated by considerations of (a) no interaction, (b) only the effect of f^* on $\dot\rho$, (c) only the effect of $\dot\rho$ on f_v^D, and (c) both interactions between void and dislocation evolution at 7954.5 hrs. As shown in this figure, a change between these distribution can be observed only in the HAZ region. Especially, the size and the value of the region with higher void fraction on the distribution become different when the type of interactions are changed. If the effect of f^* on $\dot\rho$ is only considered, the lower value of the dislocation density can be observed there. On the contrary, the similar value of the dislocation density can be observed as the case without any interactions if the effect of $\dot\rho$ on f_v^D is only included. Mixed effect of the interaction is appeared when both interactions are considered. The size of the region, where the distribution is changed, becomes smaller than the case without the effect of interactions.

5.2 Effect of grain size

Figure 11 shows creep curves obtained by the experiment and the computation in case of two different grain sizes in 5 μm and 10 μm. As can be seen, the creep curve becomes lower and the material becomes softer against the constant loading when the grain size is larger. As formulated in equation (21), a coarser grain induces the reduced rate of dislocation density. As the result, the softening behavior as shown in this figure is occurred.

Figure 12 shows distribution of void volume fraction at 7595.4 hrs calculated in case of (a) original d as shown in Table 1 and (b) twice of original d. The maximum value of the void fraction is focused upon. The maximum value decreases as the coarse grain is used. At a local region, the void fraction can be suppressed by a use of a coarser grain. This means the grain boundary effect of the void evolution can be implicitly expressed by the proposed model. Abe et al. (2007) reported that a fine-grained zone is produced in the HAZ of welded joints during heat cycle of welding, which accelerates microstructure evolution and damage development during creep at elevated temperature. This is called Type IV creep fracture. The results show a possibility of a prediction for the type IV creep fracture because of the increase in the void volume fraction with a smaller grain size.

Grain boundary diffusion and precipitates has a strong effect on the void evolution (Riedel, 1987; Khaleel et al., 2001). In near future, these effects will be included for a further precise model.
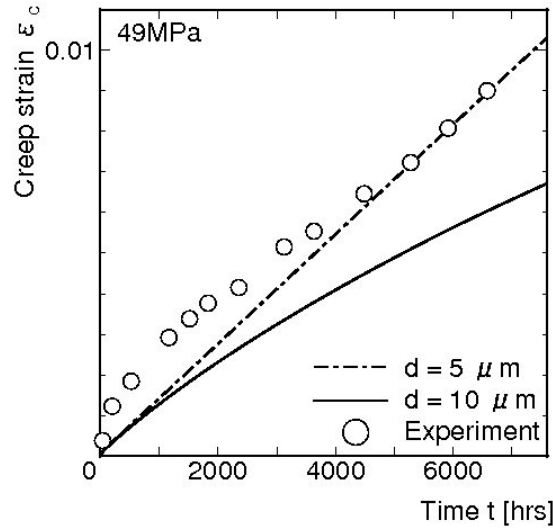
Figure 11: Creep curves obtained by the experiment and computations with two cases of grain size d

(a)   (b)

Figure 12: Distribution of void volume fraction at 7595.4 hrs calculated in the case of (a) original d as shown in Table 1 and (b) twice of original d

6 Summary

In this research work, a new framework for a numerical analysis of creep behavior including both a void evolution and a dislocation dynamics for a chrome-molybdenum steel welded joint was proposed. First, the creep constitutive model with the void evolution proposed by Takemasa et al. Takemasa et al. (1999) was generalized by vanishing the locally coupled analysis. By using the set of parameters appeared in the article (Takemasa et al., 1999), a simulation with the same condition was performed in order to compare with the computational results obtained by Takemasa et al. (1999). After that, a dislocation model, which the piled-up and annihilation are considered, proposed in the past (Mecking and Kocks, 1981; Estrin, 1998) was included into the creep constitutive equation. Interactions between the void and the dislocation were newly considered, as the void becomes an obstacle against the dislocation motion and the dense dislocation leads to the source and sink of the microvoid. All the proposed constitutive equations were implemented into the commercial software ABAQUS through the user material subroutine UMAT. The newly proposed model was verified by a comparison with the experimental result. Finally, effects of interactions and the grain size of HAZ considered here on distribution of a void fraction, a dislocation density and creep strain were examined.

Acknowledgement

References

Abe, F.; Tabuchi, M.; Kondo, M.; Tsukamoto, S.: Suppression of type IV fracture and improvement of creep strength of 9Cr steel welded joints by boron addition. *Int. J. Press. Ves. Pip.*, 84, (2007), 44 – 52.

Bao, G.: Development of high strength heat resistant materials and welding technology for 650 - 700 °C USC boilers. In: *Proc. VGB-TEMPES Technical Meeting*, Tokyo (2007).

Chu, C. C.; Needleman, A.: Void nucleation effects in biaxially stretched sheets. *Trans. ASME, J. Engng. Mater. Technol.*, 102, (1980), 249 – 256.

Estrin, Y.: Dislocation theory based constitutive modelling : foundations and appliations. *J. Mater. Proc. Technol.*, 80-81, (1998), 33 – 39.

Estrin, Y.; Mecking, H.: A unified phenomenological description of work hardening and creep based on one-parameter models. *Acta Metall.*, 32, (1984), 57 – 70.

Fujii, K.; Murao, S.; Tomita, A.; Saito, K.: Residual life evaluation of thermal power plant (RET) project - Part 1: Introduction to residual life assessment techniques and phase I of RET project. *J. Therm. Nucl. Power, Jpn.*, 498, (1998a), 1 – 17, (in Japanese).

Fujii, K.; Murao, S.; Tomita, A.; Saito, K.: Residual life evaluation of thermal power plants (RET) project - Part 2: Phase II of RET project. *J. Therm. Nucl. Power, Jpn.*, 499, (1998b), 27 – 50, (in Japanese).

Fullman, R. L.: Measurement of particle sizes in opaque bodies. *Trans. AIME*, 197, (1953), 447 – 457.

Gurson, A. L.: Continuum theory of ductile rupture by void nucleation and growth - Part I: Yield criteria and flow rules for porous ductile media. *Trans. ASME, J. Engng. Mater. Technol.*, 99, (1977), 2 – 17.

Hasegawa, S.; Maeda, Y.: Study on a creep analysis of welded part in a large-diameter piping. Tech. Rep. 76, Hokkaido Electric Power Corp. (2006), (in Japanese).

Khaleel, M. A.; Zbib, H. M.; Nyberg, E.: Constitutive modeling of deformation and damage in superplastic materials. *Int. J. Plast.*, 17, (2001), 277 – 296.

Lemaitre, J.: *A course on damage mechanics*. Springer-Verlag, Berlin (1996).

Li, H.; J., L.; Dean, T. A.; Wen, S. W.; Bannister, A. C.: Modelling mechanical property recovery of a linepipe steel in annealing process. *Int. J. Plast.*, 25, (2009), 1049 – 1065.

Lubarda, V. A.; Schneider, M. S.; Kalantar, D. H.; Remington, B. A.; Meyers, M. A.: Void growth by dislocation emission. *Acta Mater.*, 52, (2004), 1397 – 1408.

Mecking, H.; Kocks, U. F.: Kinetics of flow and strain-hardening. *Acta Metall.*, 29, (1981), 1865 – 1875.

Riedel, H.: *Fracture at high temperature*. Springer-Verlag, Berlin (1987).

Serri, J.; Cherkaoui, M.: Constitutive modeling and finite element analysis of the formability of TRIP steels. *Trans. ASME, J. Engng. Mater. Technol.*, 130, (2008), 031009.

Takemasa, F.; Suzuki, A.; Ito, K.: Creep damage analysis using the Gurson model on welded joints of mod. 9Cr-1Mo steel. In: *Trans. 15th Int. Conf. on Struct. Mech. in Reactor Technol.*, vol. X, pages 157 – 164 (1999).

Tvergaard, V.; Needleman, A.: Analysis of the cup-cone fracture in a round tensile bar. *Acta Metall.*, 32, (1984), 157 – 169.

Addresses: Assoc. Prof. Dr. Eng. Takeshi Iwamoto, Graduate School of Engineering, Hiroshima University, 1-4-1 Kagamiyama, Higashi-Hiroshima, 739-8527 Japan; Mr. Eiji Murakami, Kure Research Laboratory, Babcock-Hitachi K. K., 5-3 Takara-machi, Kure, Hiroshima, 737-0029 Japan; Prof. Dr. Eng. Toshiyuki Sawa, Graduate School of Engineering, Hiroshima University, 1-4-1 Kagamiyama, Higashi-Hiroshima, 739-8527 Japan.
email: iwamoto@mec.hiroshima-u.ac.jp; eiji.murakami.qs@hitachi.com; sawa@mec.hiroshima-u.ac.jp .